

Clean Synthetic Strategies to Biologically Active Molecules from Lignin: A Green Path to Drug Discovery**

Anastasiia M. Afanasenko, Xianyuan Wu⁺, Alessandra De Santi⁺, Walid A. M. Elgaher, Andreas M. Kany, Roya Shafiei, Marie-Sophie Schulze, Thomas F. Schulz, Jörg Haupenthal, Anna K. H. Hirsch,^{*} and Katalin Barta^{*}

Abstract: Deriving active pharmaceutical agents from renewable resources is crucial to increasing the economic feasibility of modern biorefineries and promises to alleviate critical supply-chain dependencies in pharma manufacturing. Our multidisciplinary approach combines research in lignin-first biorefining, sustainable catalysis, and alternative solvents with bioactivity screening, an in vivo efficacy study, and a structural-similarity search. The resulting sustainable path to novel anti-infective, anti-inflammatory, and anticancer molecules enabled the rapid identification of frontrunners for key therapeutic indications, including an anti-infective against the priority pathogen *Streptococcus pneumoniae* with efficacy in vivo and promising plasma and metabolic stability. Our catalytic methods provided straightforward access, inspired by the innate structural features of lignin, to synthetically challenging biologically active molecules with the core structure of dopamine, namely, tetrahydroisoquinolines, quinazolinones, 3-arylindoles and the natural product tetrahydropapaveroline. Our diverse array of atom-economic transformations produces only harmless side products and uses benign reaction media, such as tunable deep eutectic solvents for modulating reactivity in challenging cyclization steps.

Introduction

Active pharmaceutical ingredients (APIs) are essential for human well-being and represent a large and continuously growing market.^[1,2] Deriving APIs from locally available and renewable waste or side-product streams would advance circular-economy strategies by increasing the economic feasibility of modern biorefineries, and alleviate critical supply-chain dependencies in pharma manufacturing.^[3,4] Therefore, the development of creative functionalization strategies of platform chemicals, originating from emerging biorefinery concepts, to access complex, biologically active molecules, appears tremendously attractive.^[5]

Lignin, the largest renewable source of aromatics on the planet, has attracted significant attention for the sustainable

production of fuels, materials, and chemicals,^[6–8] with lesser attention devoted to fine chemicals.^[9–11] Interdisciplinary efforts to systematic API development with the intention to rapidly identify compounds of therapeutic potential from lignin, have not been undertaken. This is surprising since employing lignin in the earliest stages of drug discovery offers remarkable opportunities for the integration of the main principles of green chemistry into the manufacturing practices of pharmaceuticals—a top priority in this sector.^[11–14] Constructing complex molecules from petrochemicals typically requires multiple-step syntheses associated with high E factors,^[15] while renewable platform molecules bear sufficient structural diversity to be transformed into sophisticated scaffolds, with great synthetic efficiency and high atom-economy.^[16,17] Moreover, lignin-

[*] Dr. A. M. Afanasenko, Dr. X. Wu,⁺ Dr. A. De Santi,⁺ Prof. Dr. K. Barta
 Stratingh Institute for Chemistry, University of Groningen
 Nijenborgh 4, 9747 AG Groningen (the Netherlands)

Dr. W. A. M. Elgaher, Dr. A. M. Kany, R. Shafiei, Dr. J. Haupenthal,
 Prof. Dr. A. K. H. Hirsch
 Helmholtz Institute for Pharmaceutical Research Saarland (HIPS)-
 —Helmholtz Centre for Infection Research (HZI)
 Campus Building E8.1, 66123 Saarbrücken (Germany)
 E-mail: anna.hirsch@helmholtz-hips.de

R. Shafiei, Prof. Dr. A. K. H. Hirsch
 Saarland University, Department of Pharmacy
 Campus Building E8.1, 66123 Saarbrücken (Germany)

M.-S. Schulze, Dr. T. F. Schulz
 Institute of Virology, Hannover Medical School
 30625 Hannover (Germany)

Dr. T. F. Schulz, Prof. Dr. A. K. H. Hirsch
 Institute of Virology, Cluster of Excellence RESIST (EXC 2155),
 Hannover Medical School 30625 Hannover, (Germany)

Prof. Dr. K. Barta
 Institute for Chemistry, University of Graz
 Heinrichstrasse 28/II, 8010 Graz (Austria)
 E-mail: katalin.barta@uni-graz.at

[⁺] These authors contributed equally to this work.

[**] A previous version of this manuscript has been deposited on a preprint server (<https://doi.org/10.26434/chemrxiv-2022-b6rn4>).

© 2023 The Authors. Angewandte Chemie International Edition published by Wiley-VCH GmbH. This is an open access article under the terms of the Creative Commons Attribution License, which permits use, distribution and reproduction in any medium, provided the original work is properly cited.

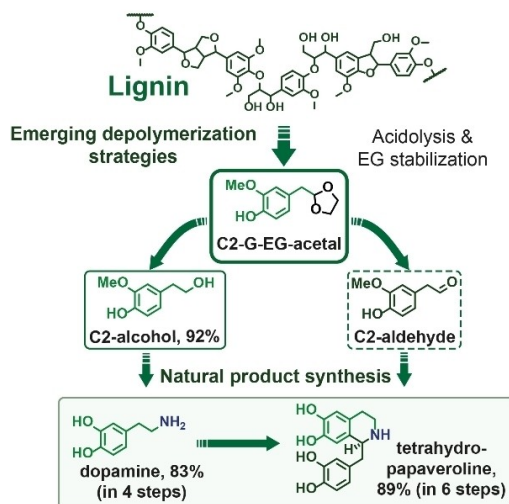
derived aromatic platform chemicals inherently incorporate structural moieties often found in naturally occurring, biologically active compounds, due to their common biosynthetic origin (see Supporting Information Section 2).^[5,18]

We hypothesized, that this constitutes an excellent starting point for the rapid access to new structurally diverse, biologically active compound libraries and rapid identification of relevant drug candidates. Hence, we set out to develop an array of atom-economic transformations to obtain synthetically challenging classes of biologically active compounds directly from **C2-G-EG-acetal**,^[19–21] a lignin-derived platform chemical (Figure 1A). As we have previously shown, this **C2-G-EG-acetal** can be obtained in near-theoretical yield from softwood lignin or lignocellulosic biomass via acidolysis and ethylene glycol stabilization, and is ideally positioned to access molecules of the dopamine platform. And indeed, by developing suitable chemocatalytic methods, and tunable deep eutectic solvents (DESS)^[22] for challenging cyclization steps, we were able to rapidly access compound libraries for biological screening. Among them, the typically synthetically challenging tetrahydroisoquinolines, quinazolinones, 3-arylindoles, dopamine itself and the natural product tetrahydropapaveroline (Figure 1A and 1B).

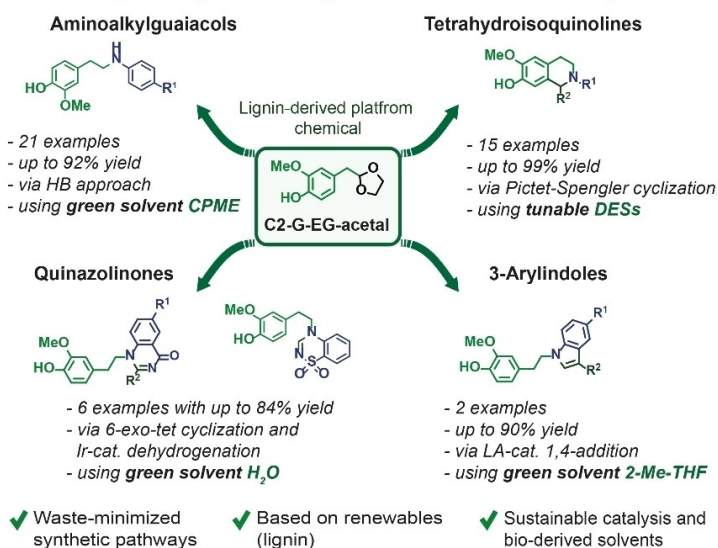
Systematic experimental screening of the obtained compound libraries for anti-infective and anticancer activities has revealed promising biological activities and further in-depth evaluation of the most promising hits led to the identification of clear frontrunners, active against highly relevant pathogens or tumor cell lines (Figure 1C). Compound **5ff** emerged as a frontrunner against *Streptococcus pneumoniae*, a priority pathogen causing human lung infections, confirmed by in vivo studies using our in-house developed *Galleria mellonella* larvae infection model. Moreover, by applying bioinformatics similarity searching to a drug library of more than 4600 compounds, we identified novel inhibitors of the anti-inflammatory target COX-2 as well as compounds with excellent antiviral activity against Kaposi's sarcoma-associated herpesvirus.

The promising biological activities, combined with the efficient and modular synthetic routes developed, demonstrate the efficiency of our interdisciplinary approach in the rapid discovery of active scaffolds from renewable resources.

A Sustainable construction of natural products from lignin-derived monomer



B Novel pathways to variety of bio-based N-heterocycles



C Rapid discovery of potential future drug candidates

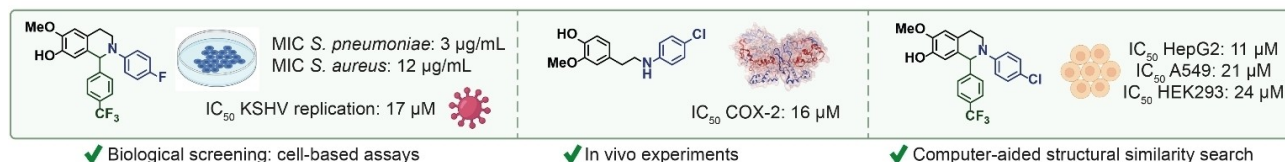


Figure 1. The green path towards novel therapeutic agents and the natural product tetrahydropapaveroline starting from lignin-derived platform chemical **C2-G-EG-acetal**. A) Overall strategy. B) Diverse classes of heterocycles synthesized from **C2-G-EG-acetal**. C) “Frontrunners” as novel pharmaceuticals in this study that display outstanding anti-infective, anti-inflammatory, and anticancer activities. Abbreviations: HB—“hydrogen borrowing”; CPME—cyclopentyl methyl ether; EG—ethylene glycol; DES—deep eutectic solvent; *S. pneumoniae*—*Streptococcus pneumoniae*; *S. aureus*—*Staphylococcus aureus*; COX—cyclooxygenase.

Results and Discussion

Direct Conversion of C2-G-EG-acetal into Homovanillyl Alcohol

The foundation of our approach is the acidolysis and ethylene glycol stabilization method pioneered in our laboratory, which leads to **C2-G-EG-acetal** in high selectivity and near theoretical yield from lignin and lignocellulose.^[19–21] Interestingly, while most cutting-edge “lignin-first” methods result in ethyl, propyl or propanol aromatics,^[23] our unique acidolysis/stabilization approach directly leads to the C2-aldehyde platform, owing to the dominance of the deformylation/C–O scission pathway through acidolysis of the β-O-4 moiety, under the conditions applied.^[24,25]

First, we have explored the direct conversion of the **C2-G-EG-acetal** into its stable C2-alcohol analogue, homovanillyl alcohol (**HA**), by the challenging deprotection/C=O hydrogenation sequence using various heterogeneous hydrogenation catalysts (Table S1). While low to moderate **HA** yields (27–63 %) were seen with Ru/C, Ru/Al₂O₃, Pd/C using *tert*-amyl alcohol as a solvent, excellent conversion and **HA** selectivity was achieved in water, presumably due to a more favorable acetal-to-aldehyde deprotection step. Particularly, employing Ru/Al₂O₃ resulted in a 98 % yield at 140 °C and with 20 bar hydrogen (Table S1, entry 5). Further optimizing the reaction conditions (5 % Ru/Al₂O₃, 20 bar H₂, 90 °C, 4.5 h), **HA** was obtained in a 92 % isolated yield (Table S1, entry 9). Next, we developed suitable hydrogen-borrowing methodologies for the direct catalytic amination of **HA** with ammonia or primary amines. Thereby, **HA** serves as a central platform to provide access to dopamine (Scheme 1B) or libraries of dopamine analogues bearing secondary amines (Figure 2A), precursors to more complex molecules.

Dopamine and Natural Product Synthesis from Lignin

The overall synthetic strategy for constructing dopamine and the natural product tetrahydropapaveroline from lignin is detailed in Scheme 1 (for more details, see Supporting Information Section 2). Hereby, we accomplished the direct coupling of **HA** with ammonia in the presence of Raney-Ni to deliver **C2-amine**, followed by demethylation to afford the target **dopamine**, in 83 % isolated yield, without the need for additional purification procedures. This constitutes a straightforward catalytic sequence from softwood lignocellulose^[21] or softwood lignin.^[19,20,26]

The subsequent formation of the core tetrahydroisoquinoline scaffold (**Me-THI**) was realized by coupling **dopamine** and **Me-C2-aldehyde**. The latter was generated in situ from the corresponding **Me-C2-EG-acetal**, which was obtained by methylation of the parent lignin platform chemical **C2-G-EG-acetal**, using the green methylation agent dimethyl carbonate (DMC). The critical Pictet–Spengler cyclization and the **Me-C2-EG-acetal** deprotection steps required the same mild, acidic reaction conditions, allowing for the development of a one-pot procedure. Finally, cleavage of the methyl ethers in **Me-THI** by hydrobromic acid afforded

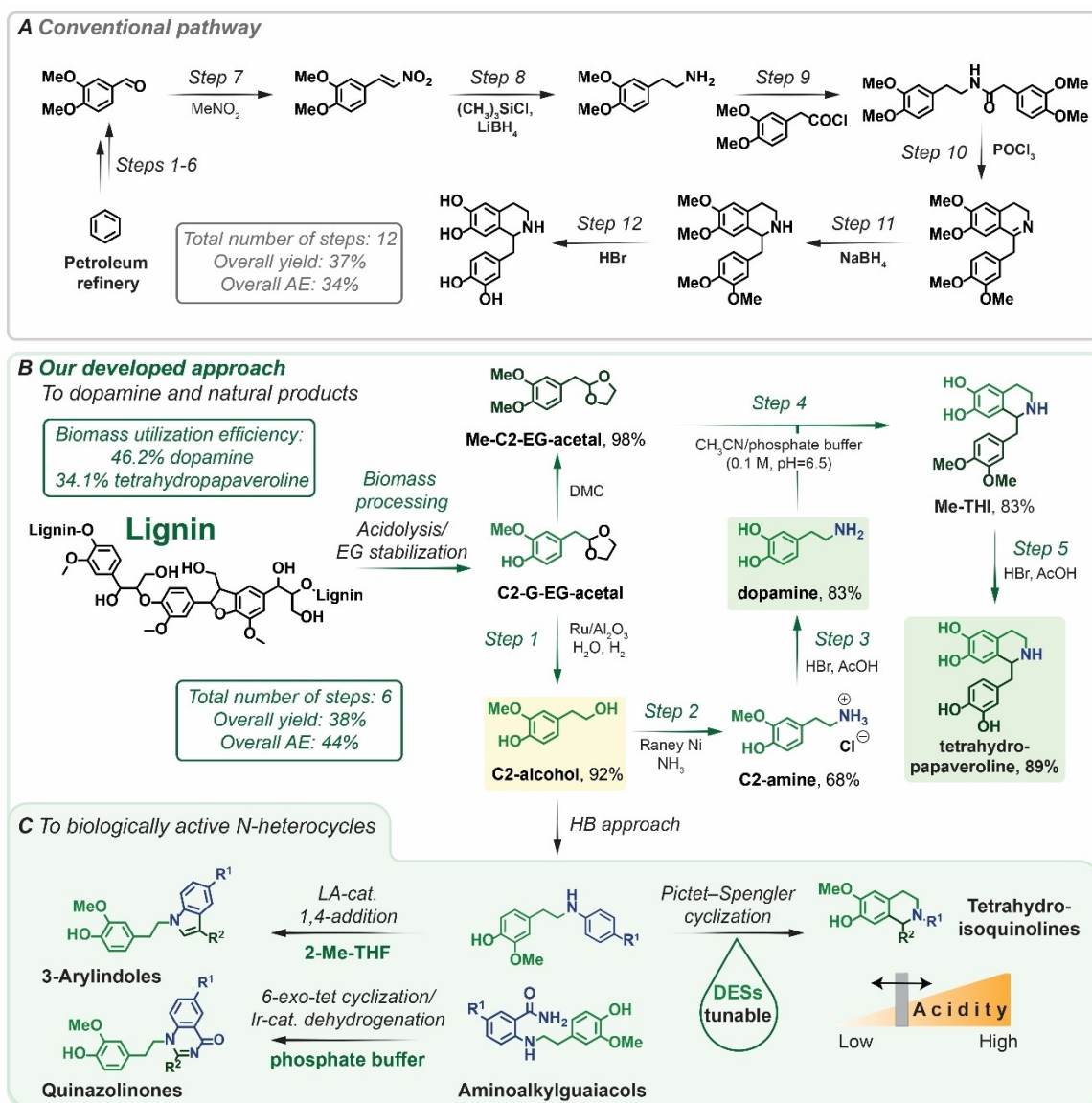
the target **tetrahydropapaveroline** in 89 % yield. While this last deprotection step is efficient and readily used in industry, there is a further need to develop chemo- or biocatalytic methods to achieve cleaner demethylation. Nonetheless, the here-developed methods clearly outperform classical synthesis routes in terms of green chemistry metrics (see Supporting Information Section 2.3). The developed sequence achieves an overall 6.24 wt % yield of dopamine and 5.65 wt % yield of **tetrahydropapaveroline**, showing high biomass utilization efficiencies (46.2 % and 34.1 %, respectively), calculated on lignin basis. In the context of developing integrated biorefinery schemes, these results are encouraging. **Dopamine**, is an *essential medicine*, widely used in the treatment of Parkinson's disease.^[27] Demonstrating scalable chemocatalytic routes to access such important and high-value targets from lignin would enhance the overall techno-economic feasibility of a biorefinery approach where all constituents of lignocellulose are effectively utilized (see Supporting Information, Note in Section 2.2).

Catalytic Conversion of HA into Aminoalkyl Guaiacol Derivatives

Having an efficient method at hand to produce **HA** from **C2-G-EG-acetal**, we aimed to create a library of dopamine derivatives for biological activity screening. The direct catalytic amination of **HA** with a range of aniline derivatives was accomplished by applying the homogeneous Ru-based Shvo's catalyst (**C1**). Gratifyingly, the catalytic coupling of **HA** with aniline, in the presence of **C1** (Table S2) outperformed in efficiency our earlier reported functionalization of dihydroconiferyl alcohol,^[16] affording the target secondary amine **3a** in perfect selectivity (99 %) and good isolated yield (74 %), using the non-toxic solvent CPME and 0.5 mol % **C1** without any additives at 120 °C (Table S2, entry 6). Further expanding the scope resulted in aminoalkyl guaiacols (Figure 2A), comprising existing structures with already known applications, as well as new structures with potential therapeutic activity. For example, the secondary amines **3b'** and **3k'** are known precursors in the synthesis of orexin receptor antagonists,^[28] used to treat sleep disorders, as well as isoalloxazine derivatives,^[29] agents for the treatment of Alzheimer's disease. Potentially, **3q** can serve as a key building block for the synthesis of medicinally relevant erythrina alkaloids.^[30,31] In our hands, the synthesized aminoalkyl guaiacols have shown various biological activities, as shown in Figure 2A and summarized in Supporting Information in Section 11.

Tunable Deep Eutectic Solvent Systems to Construct Tetrahydroisoquinolines

Next, we set out to construct variously substituted **tetrahydroisoquinolines**, via Pictet–Spengler cyclization involving the aminoalkyl guaiacols obtained above, by exploring the use of DESs for the first time in this transformation.^[22,32]



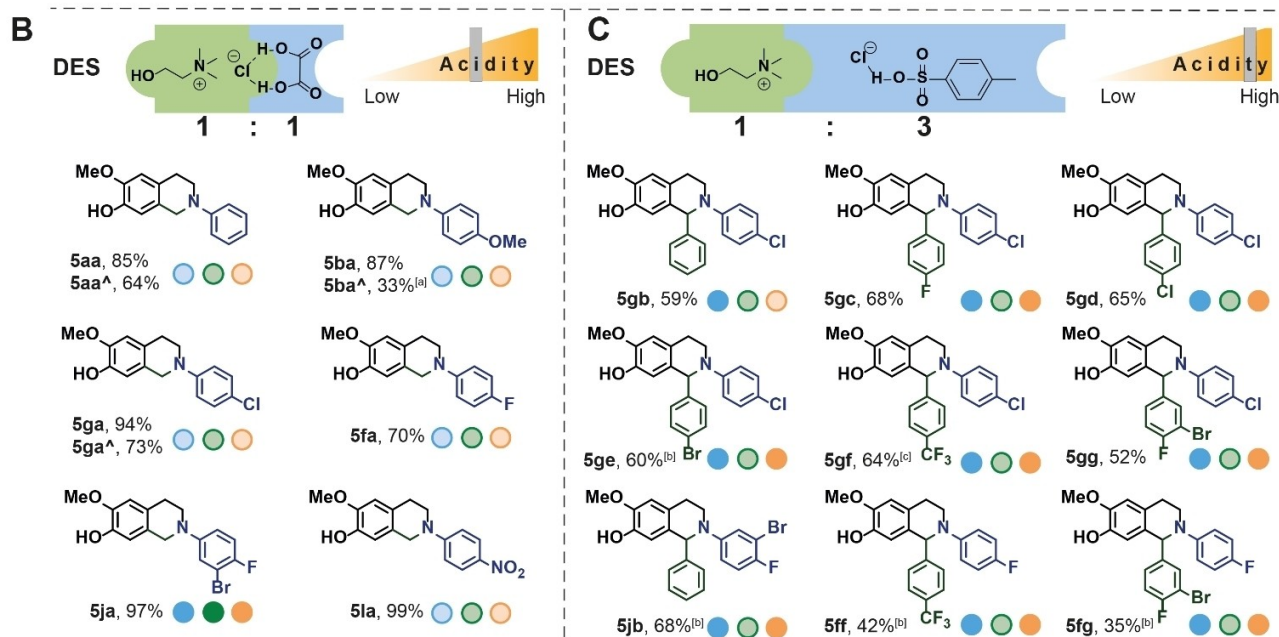
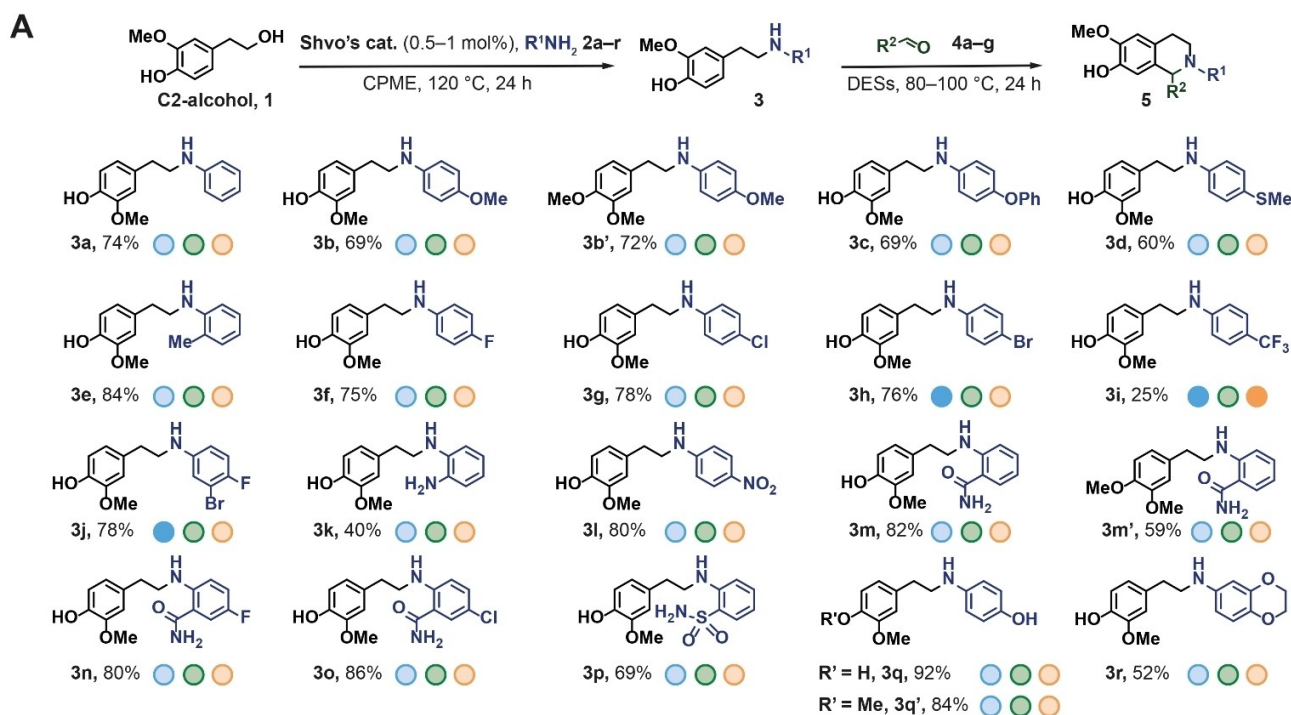
Scheme 1. Routes for the synthesis of tetrahydropapaveroline. A) Conventional path starting from benzene. B) Our chemocatalytic approach starting from lignocellulose or lignin via the aromatic platform chemical—C2-G-EG-acetal. Biomass utilization efficiencies refer to the overall process (see Supporting Information Section 2.2–2.3 for more details). Overall yield and AE are calculated starting from C2-G-EG-acetal. C) Variety of biologically active molecules that can be accessed using our developed synthetic strategies. Abbreviations: AE—atom economy; LA—Lewis acid.

Due to their favorable physicochemical properties (low vapor pressure, potentially non-toxic, biodegradable, and renewable nature), DESs are considered promising green alternatives for volatile organic solvents.^[33,34] We reasoned that this unique class of alternative reaction media will actively facilitate imine formation and accelerate the subsequent Mannich-type cyclization, both steps involved in the Pictet–Spengler mechanism.^[35] Given that these steps are sensitive both to the steric and electronic properties of the respective substrates used and the acidity of the reaction medium, we demonstrated that reactivity can be controlled through careful tuning of the DES composition, by selecting appropriate hydrogen bond donors (HBDs) and hydrogen-bond acceptors (HBAs).^[36]

We achieved high isolated yields of the tetrahydroisoquinolines (Figure 2B, **5aa–5la**, 70–99%) by coupling the aminoalkyl guaiacols (**3a–l**) with paraformaldehyde (**4a**) using natural DESs based on a combination of choline chloride (ChCl) as HBA and oxalic acid dihydrate (OA·2H₂O) as HBD.

A smooth reaction was seen at 80 °C without any strong mineral acid additives, relying solely on the beneficial effect of the DES. In comparison, moderate to good yields (Figure 2B, **5aa–5ga**, 33–73%) were achieved in a hydrochloric acid-potassium chloride buffer (0.1 M, pH 1)^[37] at a higher reaction temperature (120 °C).

However, when the synthesis of 1-substituted tetrahydroisoquinolines was attempted using 4-(2-((4-



Evaluation of Biological Activity:

Inhibitory effects on bacterial growth
Gram-positive (*Staphylococcus aureus*)

Low ● High ●

Inhibitory effects on bacterial growth
Gram-negative (*Escherichia coli*)

Low ● High ●

Inhibitory effects on the viability
of HepG2 cells

Low ● High ●

For high/low activity assessment: when tested at 100 μM - threshold 70%; at 50 μM - threshold 50%; at 25 μM - threshold 30%.

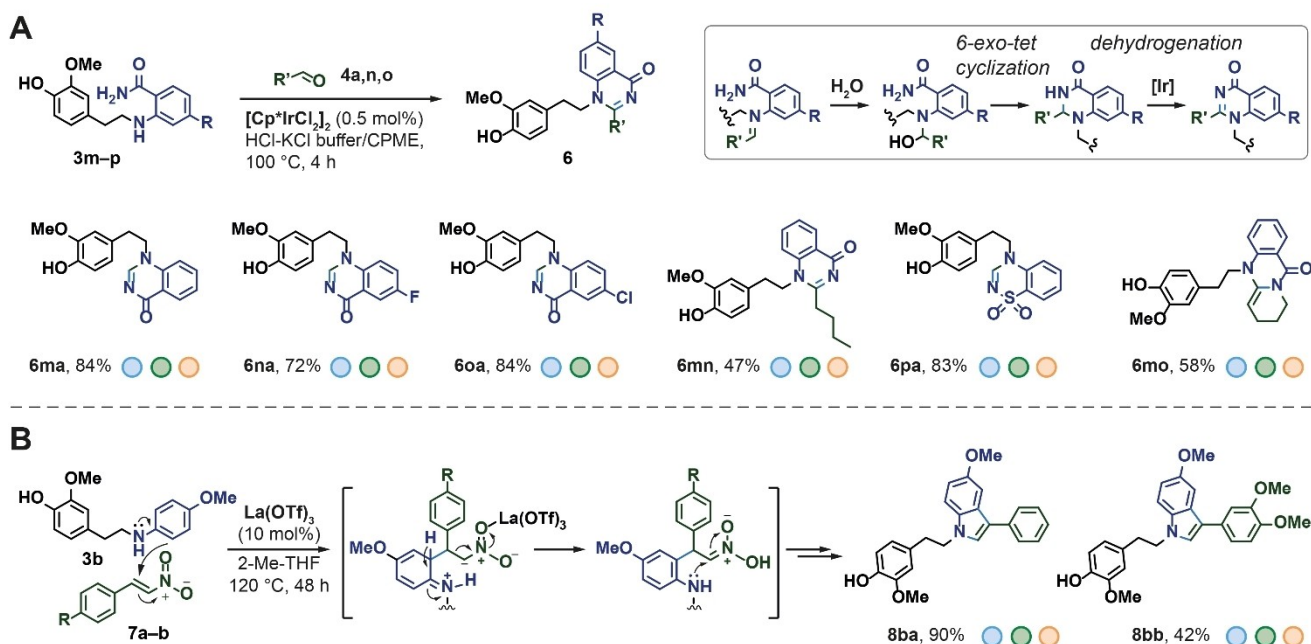
Figure 2. A) Selective ruthenium-catalyzed amination of homovanillyl alcohol with various amines. B, C) Construction of lignin-derived tetrahydroisoquinolines **5** in specific deep eutectic solvents (DESs). ^A Using HCl-KCl buffer (pH 1, 1 mL, 0.1 M)/CPME (1 mL) system instead of DESs. [a] Yield was determined by GC-FID. [b] 1.5 equiv. of the corresponding aldehyde was used. [c] 1.5 equiv. of the corresponding aldehyde was used, 80 °C.

chlorophenyl)amino)ethyl)-2-methoxyphenol (**3g**) and benzaldehyde (**4b**), the desired cyclization failed to occur in $\text{ChCl}/\text{OA}\cdot 2\text{H}_2\text{O}$ even at elevated temperature (120°C ; for more details, see Table S4). Considering the effect of the reaction medium's acidity on the efficiency of the cyclization step,^[38] we explored DESs containing choline chloride (ChCl) as HBA and strong organic acids (*p*-toluenesulfonic acid monohydrate, triflic acid) as HBD component (Table S4). The combination of choline chloride and *p*-toluenesulfonic acid monohydrate ($\text{ChCl}/p\text{-TSA}$ in a molar ratio of 1:3) at 100°C afforded the 1-substituted tetrahydroisoquinolines in exceptional selectivity with moderate to good isolated yields (Figure 2C).

Unexpected Pathways to Quinazolin-4(3H)-ones and Fully Bio-Based 3-Arylindoles

We realized that substrates **3m-p** offer a unique structural motif that would allow the construction of the quinazolinone moiety,^[39] in combination with various carbonyl compounds as coupling partners. We assumed that the iminium intermediate, formed upon the reaction of 2-aminobenzamide

and the carbonyl compound would undergo nucleophilic attack by water, via a *6-exo-tet* cyclization, followed by oxidation of the amination intermediate^[40] to deliver the desired quinazolinone scaffold. Indeed, the reaction of aminoalkyl phenol **3m** and paraformaldehyde (**4a**) using hydrochloric acid-potassium chloride buffer, at 100°C (Figure 3A) afforded the desired quinazolinone analogue. Remarkably, the target product was delivered in 64% isolated yield (Table S6, entry 1) on the first attempt. To further improve product selectivity while keeping mild reaction conditions, we were looking to enhance the reactivity by means of a catalyst. Inspired by advances in iridium-catalyzed hydrogen-transfer catalysis,^[41,42] we applied $[\text{Cp}^*\text{IrCl}_2]_2$ (Cp^* = pentamethylcyclopentadienyl) as a catalyst, presuming that it would facilitate the dehydrogenation of the formed cyclic amination.^[43] After considerable efforts, we obtained the desired *N*-heterocycle in excellent selectivity (84%) with only 0.5 mol % of $[\text{Cp}^*\text{IrCl}_2]_2$ at 100°C in 4 hours (Table S6). The scope of the reaction applying a range of 2-amino-benzamides (**3m-p**) under the established reaction conditions was examined: the target quinazolinones were delivered in high yields (**6ma-6pa**, 72–84%) without the need for any additional purification procedure (Figure 3A).



Evaluation of Biological Activity:

Inhibitory effects on bacterial growth
Gram-positive (*Staphylococcus aureus*)

Low High

Inhibitory effects on bacterial growth
Gram-negative (*Escherichia coli*)

Low High

Inhibitory effects on the viability
of HepG2 cells

Low High

For high/low activity assessment: when tested at $100\ \mu\text{M}$ - threshold 70%; at $50\ \mu\text{M}$ - threshold 50%; at $25\ \mu\text{M}$ - threshold 30%.

Figure 3. Synthesis of lignin-derived A) quinazolin-4(3H)-ones and B) *N*-substituted 3-arylindoles. General reaction conditions: A) **3m-p** (0.2 mmol, 1 equiv.), **4a** (0.22 mmol, 1.1 equiv.), $[\text{Cp}^*\text{IrCl}_2]_2$ (0.5 mol%, 0.001 mmol), HCl-KCl buffer (pH 1, 1 mL, 0.1 M) and CPME (1 mL), 100°C (temperature of the heating block), 4 h; B) **3b** (0.15 mmol, 1 equiv.), **7a,b** (0.195 mmol, 1.3 equiv.), $\text{La}(\text{OTf})_3$ (10 mol%), 2-Me-THF (2 mL), 120°C (temperature of the oil bath), 48 h.

Interestingly, using glutaraldehyde (**4o**) as a coupling partner, the pharmaceutically-relevant mackinazolinone derivative **6mo** was isolated in 58% yield.^[44] Overall, this represents the first example of obtaining quinazolinones from lignin in direct waste-minimized catalytic steps. Comparison with literature-reported conventional pathways show significant benefits in terms of green metrics (see Supporting Information Section 8.1).

Finally, we constructed *N*-substituted 3-arylidoles through the Lewis acid-catalyzed 1,4-addition of *N*-substituted anilines to *trans*- β -nitrostyrenes (Figure 3B, for more details, see Table S7). After considerable modification of the reported literature protocol,^[45] with a focus on the lignin-relevant substrates, we found that 10 mol% of La(OTf)₃ smoothly delivers the desired *N*-aryl 3-arylidole **8ba** in 90% isolated yield, in 2-Me-THF as solvent at 120 °C. This developed procedure can use vanillin-derived *trans*- β -

nitrostyrene **7b** and aminoalkyl phenol **3b**, yielding the target product **8bb** in 42% isolated yield. Considering that *p*-anisidine can also be obtained from lignin,^[46] this approach may serve as a straightforward route to construct the core scaffold of dictyodendrin alkaloids (promising telomerase inhibitors),^[47] entirely from lignin.

Evaluation of Biological Activities of the Compound Libraries

To assess the biological activities of the new lignin-based compounds, we established two approaches, namely screening of cellular activity, and innovative bioinformatics-guided similarity search (Figure 4). We screened all compounds of classes **3**, **5**, **6**, and **8** for activities against a representative Gram-positive bacterium (*Staphylococcus aureus*, Newman

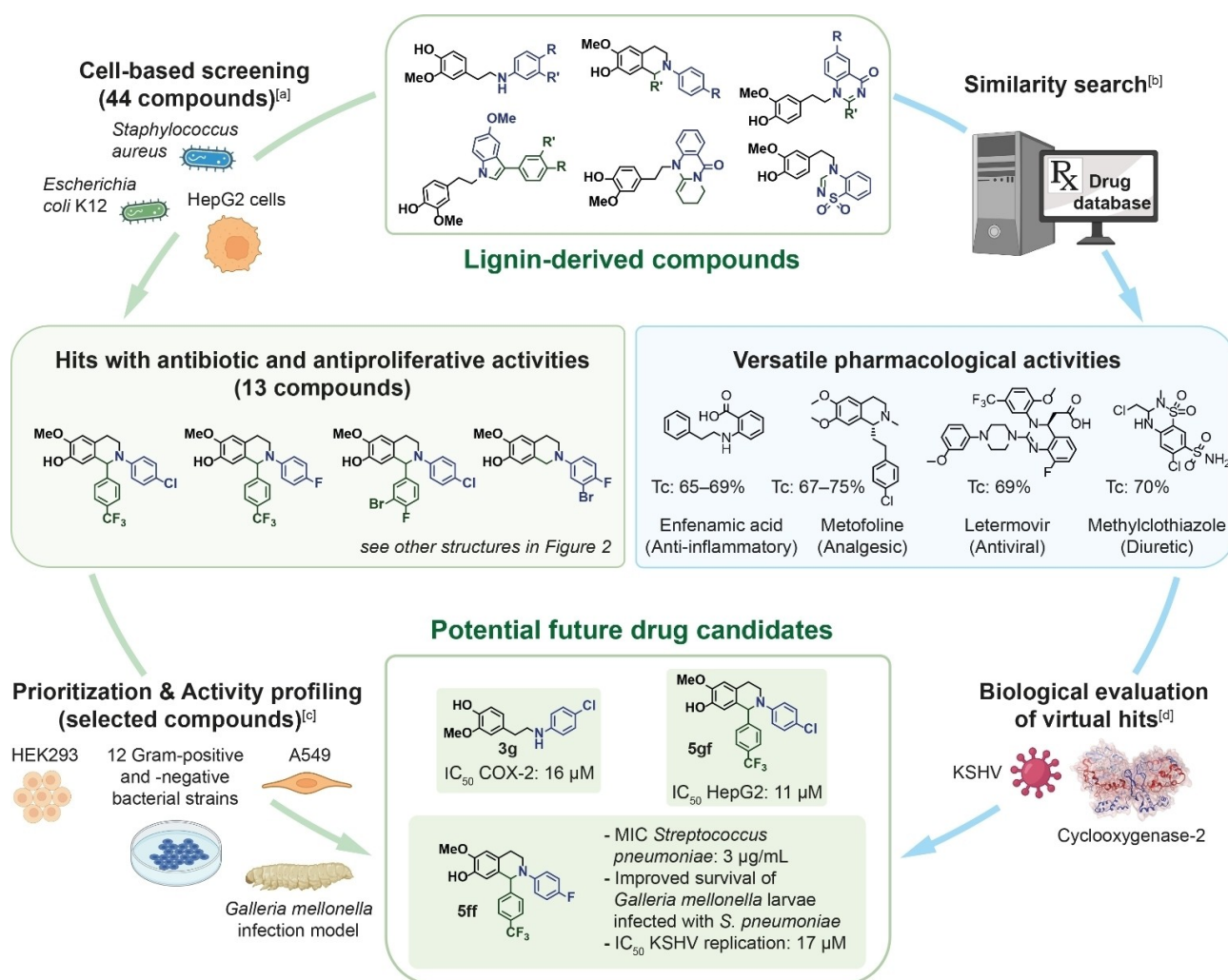


Figure 4. Identification of bioactive lignin-derived molecules through screening and similarity search strategies. Antibacterial and cytotoxicity screening yielded compounds **5ff** and **5gf** with potent activities also in an in vivo infection model based on *Galleria mellonella* larvae. The similarity assessment revealed structural similarity of the new lignin-based scaffolds to clinically approved drugs for various therapeutic indications. Evaluation of two potential pharmacological activities resulted in compounds **3g** and **5ff** with promising cyclooxygenase-2 inhibition and antiviral activity, respectively. Abbreviations: Tc—Tanimoto coefficient. Detailed results in [a] Figure S5; [b] Table S13; [c] Tables S8, S9, S10 and S12, Figures 4 and S8; [d] Table S11, Figures S6 and S7.

strain), a Gram-negative bacterium (*Escherichia coli* K12), and a human cancer cell line (HepG2 hepatoma cells).

The aminoalkyl guaiacols **3** displayed moderate growth inhibitory activities against *S. aureus* and HepG2 cells, whereas they lacked activity against *E. coli* K12 (Figure 2A and Figure S5). Compounds of the tetrahydroisoquinoline class **5** showed prominent activities against *S. aureus*, HepG2 cells, and, interestingly, *E. coli* (**5ja**; Figure 2B, 2C, and Figure S5). On the other hand, compounds of the quinazolinone **6** and indole **8** scaffolds did not show significant inhibition of bacterial growth, while they displayed moderate cytotoxic activities (Figure 3A, 3B, and Figure S5).

Next, we determined MIC and IC₅₀ values of the most active compounds (Table S8). Compound **5ja** shows promising MIC values against both *S. aureus* and *E. coli* of 12.0 ± 4.5 µg/mL and 34.3 ± 1.2 µg/mL, respectively, while compound **5ff** displayed an MIC of 11.8 ± 4.3 µg/mL against *S. aureus*.

Encouraged by these results, we tested compounds **5ja** and **5ff** against an additional 12 strains including both Gram-positive and Gram-negative pathogens of medical relevance and investigated the role of permeability and efflux for anti-Gram-negative activity (Table S9). Particularly noteworthy is the performance of compound **5ff**, which exhibits remarkable growth inhibition against all Gram-positive bacteria tested. In particular, it displays outstanding antibiotic activity against *Streptococcus pneumoniae*, as illustrated by a single-digit MIC value of 2.7 ± 0.1 µg/mL. It is worth mentioning that *S. pneumoniae* is the causative agent of pneumococcal infections and is responsible for about 1.6 million deaths every year, according to WHO estimates.^[48] This prompted us to investigate compound **5ff** in a simple and ethically uncritical in vivo model based on *G. mellonella* larvae that were infected with *S. pneumoniae* (Figure S8). Indeed, compound **5ff** showed a significant and dose-dependent improvement in the survival of the animals infected with 10⁶ CFU/larva. The administration of 250 µM resulted in a survival rate of 80 %, compared to only 35 % in the untreated control (Figure 5). These results suggest that

compound **5ff** is an effective inhibitor of *S. pneumoniae* in vitro that can also be efficacious under in vivo conditions.

Evaluation of cytotoxic activity revealed that three compounds (**5ff**, **5gf**, and **5fg**) possess IC₅₀ values in HepG2 cells below 25 µM, where **5gf** stood out with an IC₅₀ of 11.0 ± 2.0 µM. This strong effect encouraged us to investigate **5gf** in two additional human cell lines, namely lung carcinoma (A549) and human embryonic kidney (HEK293) cells. Here, the cytotoxic activity of compound **5gf** was confirmed by IC₅₀ values of 21.4 ± 1.1 µM and 24.1 ± 2.3 µM, respectively (Table S10).

Furthermore, the accessibility to many derivatives of the four classes by virtue of our straightforward synthetic methodology enabled us to study their structure–activity relationships (SARs), indicating the key structural features for activity and establishing the road for further optimization (see Supporting Information Section 11 for a detailed discussion).

Structure-Similarity Approach: Discovery of Pharmaceutically Active Compounds from Renewables

In order to identify structurally related pharmaceuticals and potentially additional biological activities of the lignin-based compounds, we carried out a chemical-similarity analysis^[49] using a drug database comprising 4,642 approved drugs (Figure 4). To cover a broad chemical space, we utilized two orthogonal fingerprints for similarity assessment of representatives of scaffolds **3**, **5**, **6**, and **8**, namely BIT_MACCS (atom connectivity) and GpiDAPH3 (pharmacophoric features). Interestingly, the new lignin-derived small molecules displayed marked similarity to several drugs having diverse pharmacological effects such as analgesic, anti-inflammatory, antibiotic, antitumor, antiviral, bronchodilator, diuretic, and neuroprotective activities (Figure 4 and Table S13). For instance, compounds **3o** and **5ga** showed similarity to the cyclooxygenase (COX) inhibitors enfenamic acid and clopirac, whereas compounds **5ff** and **6na** share structural features with letermovir, an antiviral drug against

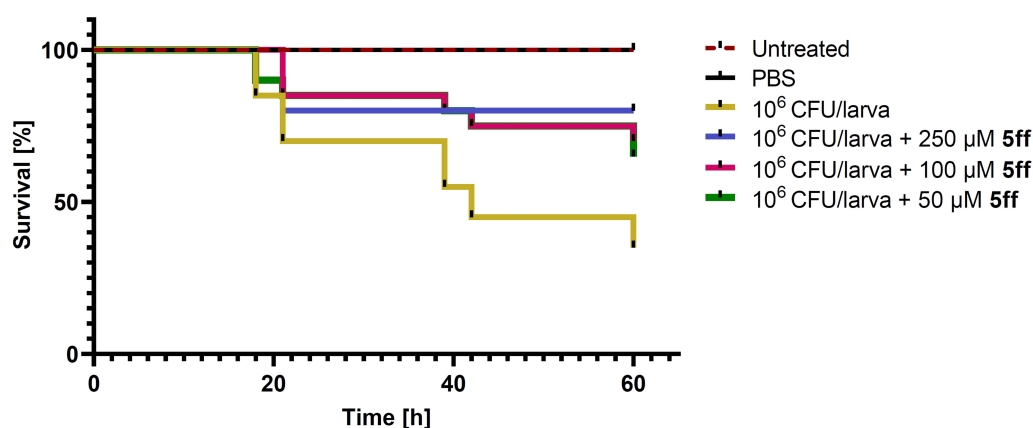


Figure 5. Kaplan–Meier survival analysis of *G. mellonella* larvae infected with 10⁶ CFU/larva of *Streptococcus pneumoniae* (strain DSM20566) in combination with compound **5ff** at several concentrations. The experiment was conducted for 3 days, and each group was monitored twice daily ($p < 0.0001$).

cytomegalovirus (CMV; Table S13). To verify these predicted activities, first, we tested nine selected compounds for COX-2 inhibition. Indeed, all compounds exhibited significant COX-2 inhibitory activities with compound **3g** showing the highest potency (IC_{50} value of $15.6 \pm 2.2 \mu\text{M}$; Table S11). In an evaluation for antiviral activity against the gamma-herpesvirus Kaposi's sarcoma-associated herpesvirus (KSHV) of compounds **3i**, **5ff**, and **6na**, compounds **3i** and **5ff** displayed a concentration-dependent inhibition of KSHV replication without affecting the viability of HEK293 host cells (Figure S6). Moreover, compound **5ff** showed an IC_{50} value of $17.4 \mu\text{M}$, which is markedly lower than that of the reference antiviral drug foscarnet ($IC_{50} = 41.7 \mu\text{M}$; Figure S7).

Given the potential of our frontrunners as novel pharmaceuticals, we determined in vitro murine metabolic and plasma stability for compounds **5ff** and **5gf** (see Table S12). In mouse liver S9 fractions, compound **5ff** demonstrated a significant metabolic stability ($t_{1/2} = 48 \pm 12$ min) similar to **5gf** ($t_{1/2} = 64 \pm 17$ min). Moreover, both compounds showed excellent plasma stability ($t_{1/2} > 240$ min). In a next step, we aim to maintain the excellent metabolic and plasma stability while aiming to achieve submicromolar IC_{50} values by structural modifications. This should be accompanied by good selectivity against relevant human off-targets and low cytotoxicity.

Conclusions

In this contribution, we adequately demonstrate that the valuable aromatic scaffold of lignin, originating from the amino acids phenylalanine and tyrosine,^[18] represents an excellent basis for the development of novel sustainable and scalable chemocatalytic strategies for the synthesis of known natural products as well as various classes of biologically active compounds based on the dopamine scaffold. The methods introduced allow straightforward access to structurally diverse molecule libraries without the formation of harmful side products and avoid the use of classical volatile and toxic solvents. The newly developed catalytic pathways were compared to classical synthesis routes in terms of green metrics, showing clear advantages (see Supporting Information Sections 2.3, 8.1 and 9.1).

Remarkably, our approach has generated several novel scaffolds with diverse activity ranging from antibacterial over antiproliferative to antiviral. Given their balanced profiles in terms of no cytotoxicity paired with high activity and stability, these new frontrunners open the door for further development of novel therapeutics to treat various indications, including the currently neglected infectious diseases. Here, rapid access to advanced molecular starting points is even more crucial than for other diseases.

By providing creative strategies for the construction of relevant biologically active scaffolds from biomass depolymerization products, guided by cellular activity and chemical similarity search methods, this contribution provides a clear way forward for the integration of green manufacturing practices in the discovery of novel therapeutic agents, at the

same time enabling the defossilization of the pharmaceutical industry. With lignocellulosic biorefineries gaining increasing importance in efforts to reduce our dependence on petroleum,^[3] this strategy opens new possibilities towards high-end and high-value target molecules, which are essential to increase the overall economic feasibility of such biorefineries.

Supporting Information

The authors have cited additional references within the Supporting Information.

Acknowledgements

The authors thank J. Jung, S. Amann and S. Wolter for excellent technical support. A. K. H. H. is thankful for financial support from Helmholtz Association's Initiative and Networking Fund and ERC starting grant 757913. K. B. is grateful for financial support from the European Research Council, ERC Starting Grant 2015 (CatASus) 638076. This work is part of the research program Talent Scheme (Vidi) with project number 723.015.005, which is partly financed by The Netherlands Organization for Scientific Research (NWO). X. W. is grateful for financial support from the China Scholarship Council (grant number 201808330391).

Conflict of Interest

The authors declare no conflict of interest.

Data Availability Statement

The data that support the findings of this study are available in the supplementary material of this article.

Keywords: Dopamine • Drug Discovery • Green Chemistry • Lignin • Tunable Deep Eutectic Solvents

- [1] "Active Pharmaceutical Ingredients Market Report, 2021–2028, Grand View Research, <https://www.grandviewresearch.com/industry-analysis/active-pharmaceutical-ingredientsmarket>".
- [2] J. Park, M. A. Kelly, J. X. Kang, S. S. Seemakurti, J. L. Ramirez, M. C. Hatzell, C. Sievers, A. S. Bommarium, *Green Chem.* **2021**, *23*, 7488–7498.
- [3] W. Lan, J. S. Luterbacher, *ACS Cent. Sci.* **2019**, *5*, 1642–1644.
- [4] J. Domínguez-Robles, Á. Cárcamo-Martínez, S. A. Stewart, R. F. Donnelly, E. Larrañeta, M. Borrega, *Sustainable Chem. Pharm.* **2020**, *18*, 100320.
- [5] A. Afanasenko, K. Barta, *iScience* **2021**, *24*, 102211.
- [6] A. Rahimi, A. Ulbrich, J. J. Coon, S. S. Stahl, *Nature* **2014**, *515*, 249–252.

- [7] A. J. Ragauskas, G. T. Beckham, M. J. Biddy, R. Chandra, F. Chen, M. F. Davis, B. H. Davison, R. A. Dixon, P. Gilna, M. Keller, et al., *Science* **2014**, *344*, 1246843.
- [8] C. O. Tuck, E. Pérez, I. T. Horváth, R. A. Sheldon, M. Poliakoff, *Science* **2012**, *337*, 695.
- [9] X. Chen, S. Song, H. Li, G. Gözaydın, N. Yan, *Acc. Chem. Res.* **2021**, *54*, 1711–1722.
- [10] Z. Mycroft, M. Gomis, P. Mines, P. Law, T. D. H. Bugg, *Green Chem.* **2015**, *17*, 4974–4979.
- [11] “Synthesis of Paracetamol (Acetaminophen) from Biomass-Derived P-Hydroxybenzamide”: J. Ralph, S. Karlen, J. Mobley, US 10286504 B2, **2019**.
- [12] H. Sneddon, *Future Med. Chem.* **2014**, *6*, 1373–1376.
- [13] M. C. Bryan, P. J. Dunn, D. Entwistle, F. Gallou, S. G. Koenig, J. D. Hayler, M. R. Hickey, S. Hughes, M. E. Kopach, G. Moine, et al., *Green Chem.* **2018**, *20*, 5082–5103.
- [14] United Nations, Department of Economic and Social Affairs, Sustainable Development, “National strategies and SDG integration”.
- [15] R. A. Sheldon, *Green Chem.* **2017**, *19*, 18–43.
- [16] S. Elangovan, A. Afanasenko, J. Hauptenthal, Z. Sun, Y. Liu, A. K. H. Hirsch, K. Barta, *ACS Cent. Sci.* **2019**, *5*, 1707–1716.
- [17] Z. Sun, G. Bottari, A. Afanasenko, M. C. A. Stuart, P. J. Deuss, B. Fridrich, K. Barta, *Nat. Catal.* **2018**, *1*, 82–92.
- [18] W. Boerjan, J. Ralph, M. Baucher, *Annu. Rev. Plant Biol.* **2003**, *54*, 519–546.
- [19] P. J. Deuss, M. Scott, F. Tran, N. J. Westwood, J. G. De Vries, K. Barta, *J. Am. Chem. Soc.* **2015**, *137*, 7456–7467.
- [20] P. J. Deuss, C. W. Lahive, C. S. Lancefield, N. J. Westwood, P. C. J. Kamer, K. Barta, J. G. de Vries, *ChemSusChem* **2016**, *9*, 2974–2981.
- [21] A. De Santi, M. V. Galkin, C. W. Lahive, P. J. Deuss, K. Barta, *ChemSusChem* **2020**, *13*, 4468–4477.
- [22] E. L. Smith, A. P. Abbott, K. S. Ryder, *Chem. Rev.* **2014**, *114*, 11060–11082.
- [23] M. V. Galkin, J. S. M. Samec, *ChemSusChem* **2016**, *9*, 1544–1558.
- [24] Y. M. Questell-Santiago, M. V. Galkin, K. Barta, J. S. Luterbacher, *Nat. Chem. Rev.* **2020**, *4*, 311–330.
- [25] A. De Santi, S. Monti, G. Barcaro, Z. Zhang, K. Barta, P. J. Deuss, *ACS Sustainable Chem. Eng.* **2021**, *9*, 2388–2399.
- [26] P. J. Deuss, C. S. Lancefield, A. Narani, J. G. De Vries, N. J. Westwood, K. Barta, *Green Chem.* **2017**, *19*, 2774–2782.
- [27] A. C. Whitfield, B. T. Moore, R. N. Daniels, *ACS Chem. Neurosci.* **2014**, *5*, 1192–1197.
- [28] “Monoamide Derivatives as Orexin Receptor Antagonists”: H. Knust, M. Nettekoven, E. Pinard, O. Roche, M. Rogers-Evans, WO 2009/016087 A1, **2009**.
- [29] A. M. Kanhed, A. Sinha, J. Machhi, A. Tripathi, Z. S. Parikh, P. P. Pillai, R. Giridhar, M. R. Yadav, *Bioorg. Chem.* **2015**, *61*, 7–12.
- [30] J. Liang, J. Chen, J. Liu, L. Li, H. Zhang, *Chem. Commun.* **2010**, *46*, 3666–3668.
- [31] Z. Q. Pan, J. X. Liang, J. B. Chen, X. D. Yang, H. Bin Zhang, *Nat. Prod. Bioprospect.* **2011**, *1*, 129–133.
- [32] S. Handy, M. Wright, *Tetrahedron Lett.* **2014**, *55*, 3440–3442.
- [33] F. Jérôme, R. Luque, *Bio-Based Solvents* **2017**.
- [34] Q. Zhang, K. De Oliveira Vigier, S. Royer, F. Jérôme, *Chem. Soc. Rev.* **2012**, *41*, 7108–7146.
- [35] J. Stöckigt, A. P. Antonchick, F. Wu, H. Waldmann, *Angew. Chem. Int. Ed.* **2011**, *50*, 8538–8564.
- [36] Y. Liu, N. Deak, Z. Wang, H. Yu, L. Hameleers, E. Jurak, P. J. Deuss, K. Barta, *Nat. Commun.* **2021**, *12*, 5424.
- [37] T. Pesnot, M. C. Gershater, J. M. Ward, H. C. Hailes, *Chem. Commun.* **2011**, *47*, 3242–3244.
- [38] A. Yokoyama, T. Ohwada, K. Shudo, *J. Org. Chem.* **1999**, *64*, 611–617.
- [39] I. Khan, A. Ibrar, W. Ahmed, A. Saeed, *Eur. J. Med. Chem.* **2015**, *90*, 124–169.
- [40] N. Y. Kim, C. H. Cheon, *Tetrahedron Lett.* **2014**, *55*, 2340–2344.
- [41] D. Wang, D. Astruc, *Chem. Rev.* **2015**, *115*, 6621–6686.
- [42] A. Bartoszewicz, N. Ahlsten, B. Martín-Matute, *Chem. Eur. J.* **2013**, *19*, 7274–7302.
- [43] J. Zhou, J. Fang, *J. Org. Chem.* **2011**, *76*, 7730–7736.
- [44] A. O. Nasrullaev, Z. E. Turdibaev, B. Z. Elmuradov, A. Yili, H. A. Aisa, K. M. Shakhidoyatov, *Chem. Nat. Compd.* **2012**, *48*, 638–642.
- [45] R. Gattu, S. Bhattacharjee, K. Mahato, A. T. Khan, *Org. Biomol. Chem.* **2018**, *16*, 3760–3770.
- [46] E. Blondiaux, J. Bomon, M. Smoleń, N. Kaval, F. Lemièrre, S. Sergeev, L. Diels, B. Sels, B. U. W. Maes, *ACS Sustainable Chem. Eng.* **2019**, *7*, 6906–6916.
- [47] W. Zhang, J. M. Ready, *Nat. Prod. Rep.* **2017**, *34*, 1010–1034.
- [48] “Pneumococcal conjugate vaccines. WHO, retrieved on the 15th of March 2022; <https://www.who.int/teams/health-product-policy-and-standards/standards-and-specifications/vaccines-quality/pneumococcal-conjugate-vaccines>”.
- [49] G. Maggiora, M. Vogt, D. Stumpfe, J. Bajorath, *J. Med. Chem.* **2014**, *57*, 3186–3204.

Manuscript received: June 9, 2023

Accepted manuscript online: October 15, 2023

Version of record online: November 14, 2023